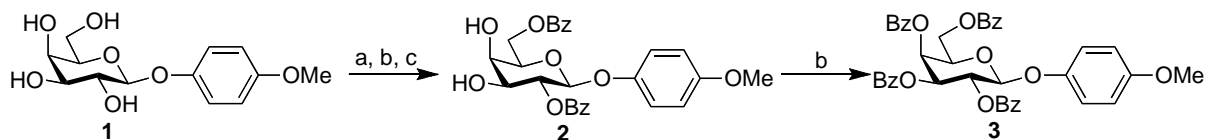


SUPPORTING INFORMATION

Phase selective carbohydrate gelator

Somnath Mukherjee* and Balaram Mukhopadhyay*

Synthesis and characterization of *p*-Methoxyphenyl 2,6-di-*O*-benzoyl- β -D-galactopyranoside (**2**):



Scheme S1: Synthesis of the amphiphile **2** and compound **3**

Reagents and condition: a. Acetone, H₂SO₄-silica; b. BzCl, Py; c. MeOH, H₂SO₄-silica

To a solution of known, *p*-methoxyphenyl β -D-galactopyranoside (**1**)¹ (3.0 g, 10.5 mmol) in dry acetone (15 mL) was added H₂SO₄-silica² (100 mg) and the mixture was stirred at room temperature for 2 hours when TLC (1:1, *n*-hexane-EtOAc) showed complete consumption of the starting material. Pyridine (7.5 mL) was added followed by BzCl (3.7 mL, 31.5 mmol) and the mixture was stirred at room temperature for 2 hours. The solvents were evaporated *in vacuo* and co-evaporated with toluene. The residue was dissolved in MeOH (15 mL), H₂SO₄-silica (100 mg) was added and the mixture was stirred at room temperature for 2 hours. Then the mixture was neutralized by Et₃N and the solvents were evaporated *in vacuo*. The residue was purified by flash chromatography using *n*-hexane-EtOAc (1:1) to afford pure compound **2** (3.6 g, 70%). ¹H NMR (500 MHz, CDCl₃) δ : 7.58-6.63 (m, 14H, ArH), 5.48 (t, 1H, *J* 7.0 Hz, H-2), 5.00 (d, 1H, *J* 8.0 Hz, H-1), 4.72 (dd, 1H, *J* 5.0 Hz, 12.5 Hz, H-6a), 4.67 (dd, 1H, *J* 7.5 Hz, 12.5 Hz, H-6b), 4.12 (d, 1H, *J* 3.0 Hz, H-4), 4.00 (dd, 1H, *J* 6.5 Hz, 8.5 Hz, H-5), 3.94 (dd, 1H, *J* 3.0 Hz, 8.5 Hz, H-3), 3.70 (s, 3H, C₆H₄OCH₃). ¹³C NMR (125 MHz, CDCl₃) δ : 167.3, 166.5 (2 \times COPh), 155.5, 151.2, 133.5, 133.3, 129.9(2), 129.8(2), 129.6, 129.4, 128.4(4), 118.8(2), 114.4(2) (ArC), 100.7 (C-1), 74.0, 72.8, 72.6, 68.7, 63.2, 55.5 (C₆H₄OCH₃). HRMS calcd for C₂₇H₂₆O₉Na (M+Na)⁺: 517.1475, found: 517.1469.

1. Z. Zhang, G. Magnusson, *J. Org. Chem.*, **1996**, *61*, 2383-2393.
2. **Preparation of H₂SO₄-silica:** To a slurry of silica gel (10 g, 200-400 mesh) in dry diethyl ether (50 mL) was added commercially available conc. H₂SO₄ (1 mL) and shaken for 5 min. Solvent were evaporated under reduced pressure resulting free flowing H₂SO₄-silica. It was then dried at 110 °C for 3 hours and used for the reaction.

Gelation and Gel Characterization

Required amount of the gelator and measured amount of pure solvent were placed in a screw-capped vial with internal diameter (i.d) of 10 mm and slowly heated until the gelator was completely dissolved. Then the solution was cooled to room temperature to form the gels. The vials were inverted to see the formation of the gel (**Figure S1**). Minimum Gelation Concentration (MGC) was calculated as described in the literature.³ All of the gels were found to be thermally reversible. Upon heating above their gelation temperature they became solution and, returned to their original gel state upon cooling.

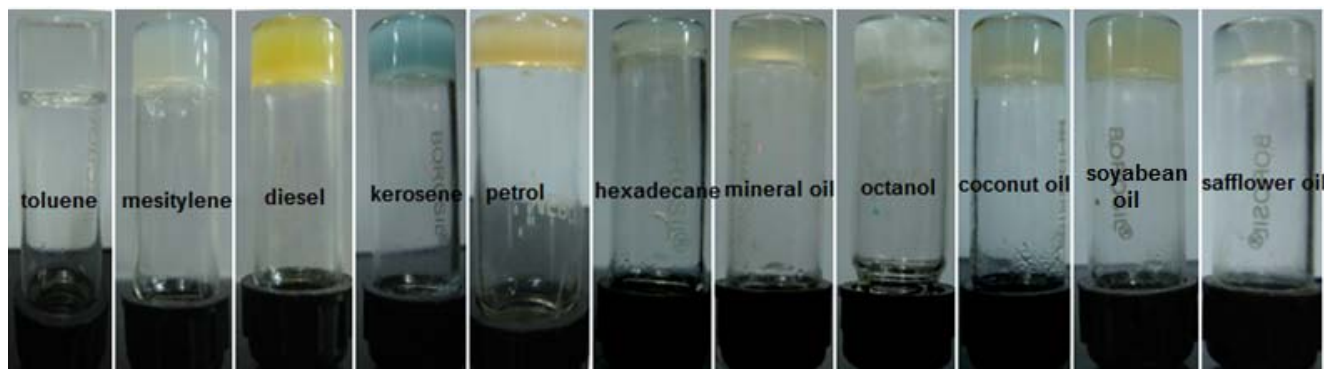
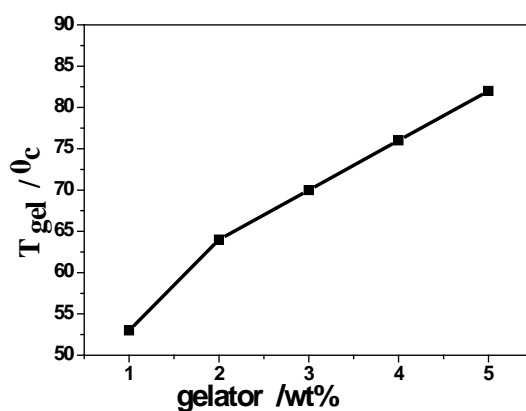


Figure S1: Photograph of the gels of compound **2** in different solvents

Determination of gel-sol transition temperature (T_{gel}): The gel-to-sol transition temperature (T_{gel}) was determined by placing the organogel containing screw-capped glass vial (i.d. = 10 mm) into a thermostated oil bath and it was gradually heated and temperature observed. The temperature at which the gel melted to solution was recorded as T_{gel} . Above the melting point the gel converts to solution, upon cooling below T_{gel} it forms the gel (**Figure S2**).



3. K. Hanabusa, M. Yamada, M. Kimura and H. Shirai, *Angew. Chem. Int. Ed.* **1996**, 35, 1949.

Figure S2: Plot of gel-sol transition temperature (T_{gel}) against gelator concentration of toluene gel of compound **2**

Microscopic studies: The self-assembled morphologies of the gelator in various solvents were investigated by the Field Emission Scanning Electron Microscopy (FE-SEM), Transmission Electron Microscopy (TEM), Atomic Force Microscopy (AFM) and Differential Interference Contrast (DIC) image. FE-SEM images show fibrous morphologies of the thermo reversible gelators in various solvents. However, size and nature of the of the fibres are not same in different solvents. Toluene gel shows (**Figure S3a**) three dimensional networks formed by cross linked self assembled nano fibres approximately 30-50 nm in diameter and several micrometer long and which probably point towards the entrapment of the solvent molecules into the spaces in the 3D network.⁴ In case of *p*-xylene (**Figure S3d**), benzene (**Figure S3b**) and kerosene (**Figure S3e**), somewhat stiff fibrous morphologies are observed and these are approximately 300-340 nm, 280-340 nm and 320-400 nm in diameter respectively. FE-SEM image of the organogelator in mesitylene (**Figure S3c**) shows spiral fibre type of morphologies and those are approximately 80-190 nm in diameter. The TEM micrograph of the gelator in toluene (**Figure S3g**) showed the cross linked fibre structure of the gelator in which fibres are approximately 30-50 nm in diameter and that was comparable to the corresponding SEM image. The morphology of the organogels were further confirmed from the AFM. AFM image of the gelator in toluene also support the cross linked fibrous Morphology, in which fibres are approximately 30-60 nm in diameter and several micrometer in length. AFM images of the organogelator in *p*-xylene, *m*-xylene, chlorobenzene, bromobenzene and *o*-xylene also exhibit cross linked fibres approximately 290-310 nm, 40-60 nm, 30-50 nm, 40-90 nm, and 40-75 nm in diameter respectively (**Figure S4**). Organogelator in mesitylene shows spiral fibre type of morphology approximately 60-170 nm in diameter. DIC image of the diesel gel was taken and it shows cross linked fibrous morphology in which fibres are about 700 nm in diameter and several micrometer in length.

FE-SEM was performed using JEOL-6700F microscope. A piece of gel was mounted on a glass slide and coated with platinum for SEM sampling and dried for a few hours under vacuum for imaging. The morphology of the dried gels was studied by using AFM (NTMDT instrument, modelAP0100) in semicontact mode. A piece of gel was mounted on clean microscope cover glass and dried for a few hours under vacuum before imaging. TEM was performed using JEOL JEM 2100 microscope and 0.08% wt/vol solution that is near to the MGC was placed on a copper grids for TEM sampling. Then it was dried for few hours under vacuum for imaging. For getting DIC image of the gelator in diesel (1.2% wt/vol), a

4. (a) M. Suzuki, Y. Nakajima, M. Yumoto, M. Kimura, H. Shirai, K. Hanabusa, *Langmuir* **2003**, *19*, 8622-8624. (b) S. Debnath, A. Shome, S. Dutta, P. K. Das, *Chem. Eur. J.* **2008**, *14*, 6870-6881.

small piece of gel in diesel was placed on a glass slide and dried for few hours for imaging, then DIC image was taken using inverted fluorescence microscopy (IX 81, Olympus).

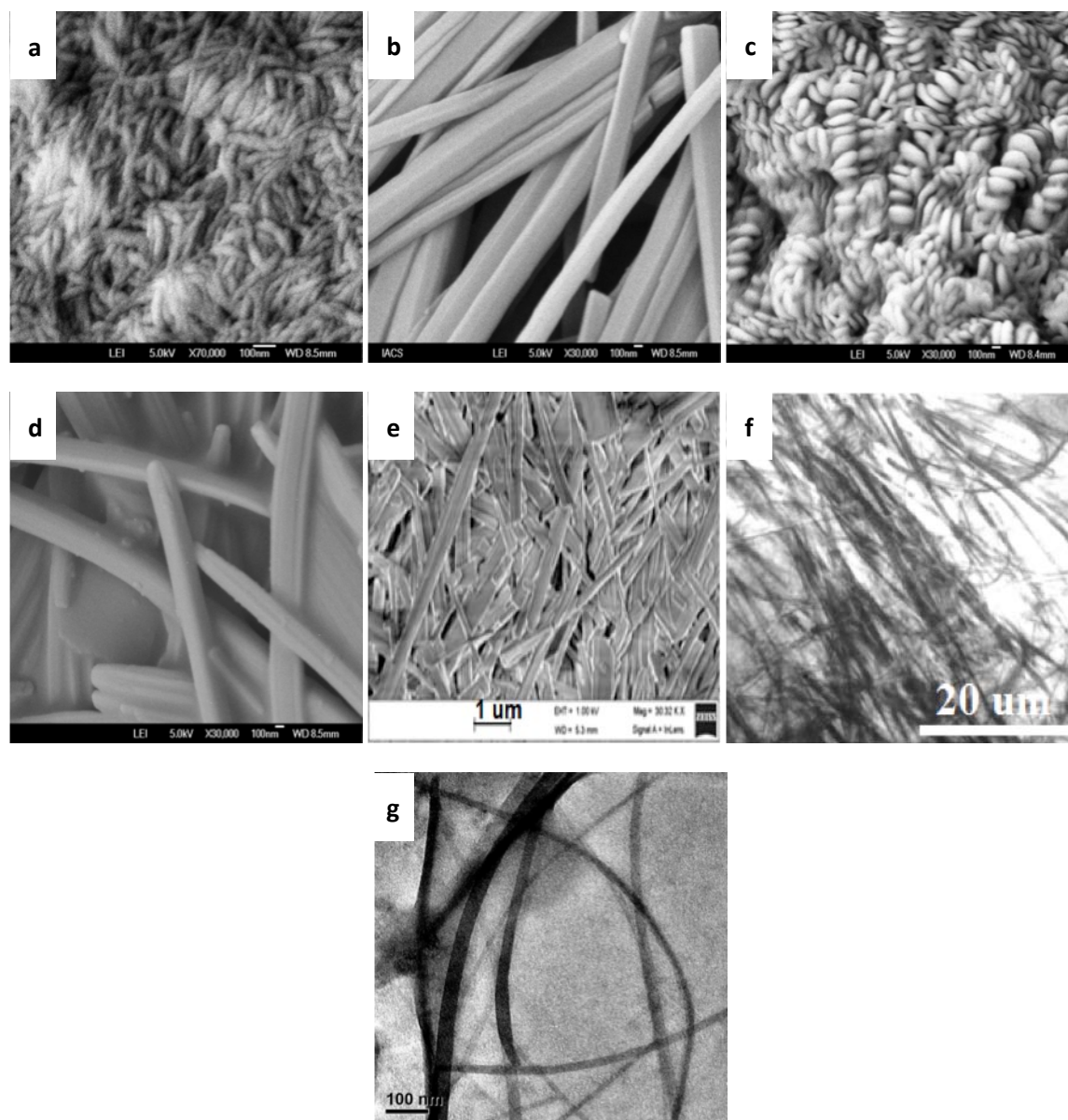


Figure S3: FE-SEM images of the (a) toluene gel, (b) benzene gel, (c) mesitylene gel, (d) *p*-xylene gel, (e) SEM image of kerosene gel at MGC, (f) DIC image of the diesel gel (3% wt/v) (wt/v) (g) TEM image of the gelator in toluene (0.08%wt/v)

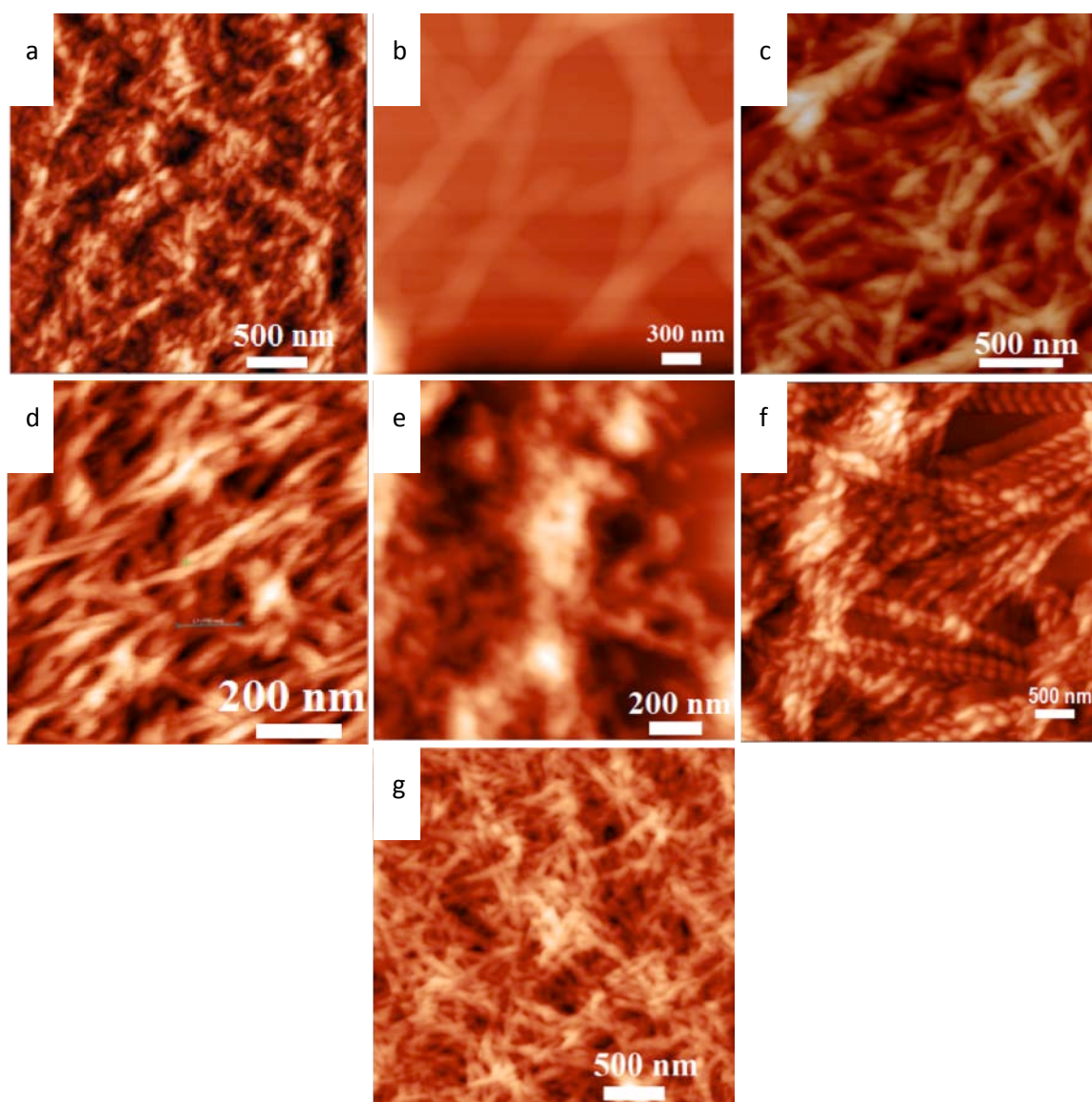


Figure S4: AFM images of the gelator in (a) toluene, (b) *p*-xylene, (c) *o*-xylene (d) *m*-xylene (e) petrol (f) mesitylene (g) bromobenzene at MGC

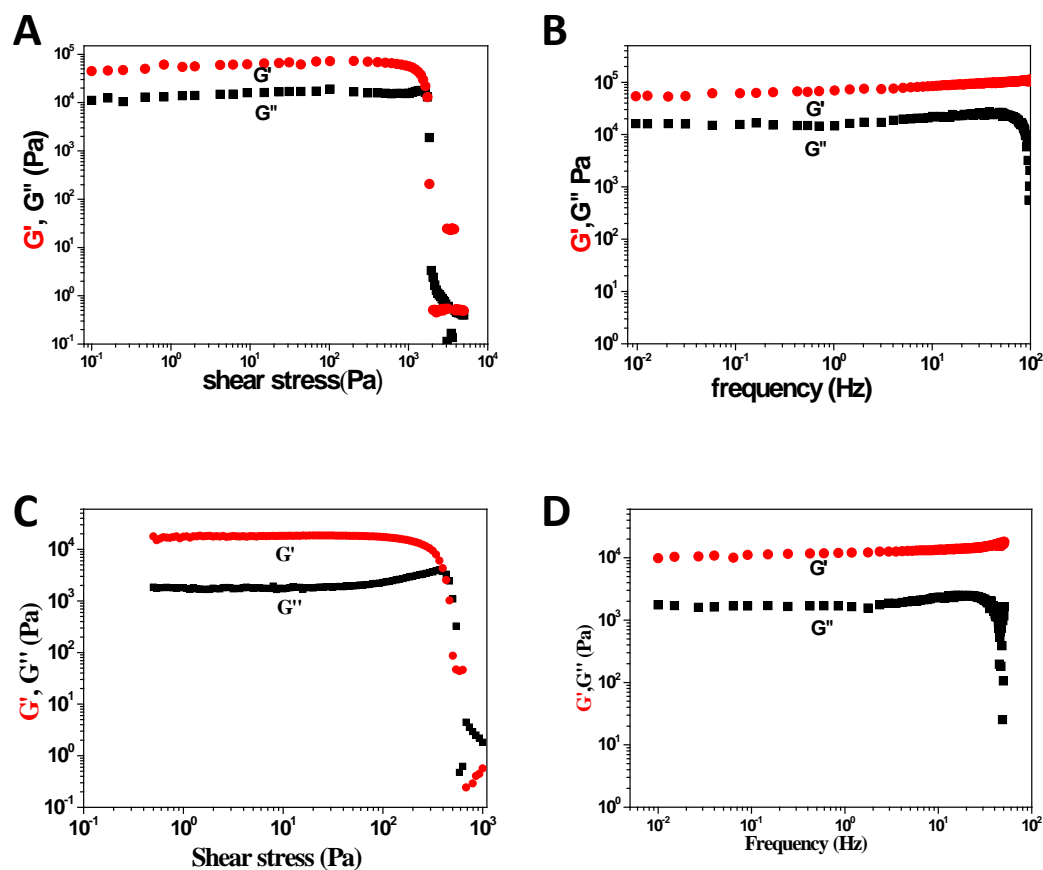


Figure S5: Rheological studies for toluene gel (2% wt/v) (a) stress sweep (b) frequency sweep; Rheological studies for mesitylene gel (2% wt/v) (c) stress sweep (d) frequency sweep

Rheological studies: Rheological measurements were performed using Bohlin Make Gemini rheometer equipped with steel coated parallel-plate geometry (40 mm diameter). The gap distance was fixed at 500 μ m. A solvent-trapping device was placed above the plate to avoid evaporation. All measurements were made at 25 °C. All the gels were prepared and allowed to set for 1 hour. A small portion of the set gel was placed on the smooth plate of the rheometer and the parallel-plate geometry was lowered to its truncation gap, and the gel was allowed to equilibrate for 10 minutes before starting the experiment. First, a stress sweep at fixed frequency (1 Hz) allowed determination of the linear regime of the sample. This was made by measuring the storage modulus G' and the loss modulus G'' as a function of the stress amplitude. Second, the frequency sweep was obtained over the frequency range at a constant strain of 0.01% (**Figure S5**).

Powder X-Ray Diffraction (PXRD): The PXRD patterns of the solid powdered compound and xerogel of toluene (1%wt/v) were collected on a Rigaku SmartLab with a Cu $K\alpha$ radiation (1.540 Å). The tube voltage and amperage were set at 40 kV and 50 mA respectively. Each sample was scanned between 3° and 40 (2 θ) with a step size of 0.02°. The instrument was previously calibrated using a silicon standard. The xerogel diffraction signal significantly differs from the powdered compound. The results are listed in **Table S1**. As shown in **Figure S6**, xerogel exhibit three major reflection peaks in the small angle region (2 theta = 3 to 16 degree) and the corresponding d spacings (15.95 Å, 7.15 Å, 5.85 Å) follow the ratio about 1:1 /2:1/3, indicating that xerogel posses a layered structure and interlayer distance is 15.95 Å which is closed to the calculated molecular length (17.15 Å) of galactoside 2. Other peaks in the high angle region may relate to the intermolecular stacking distances in three directions.

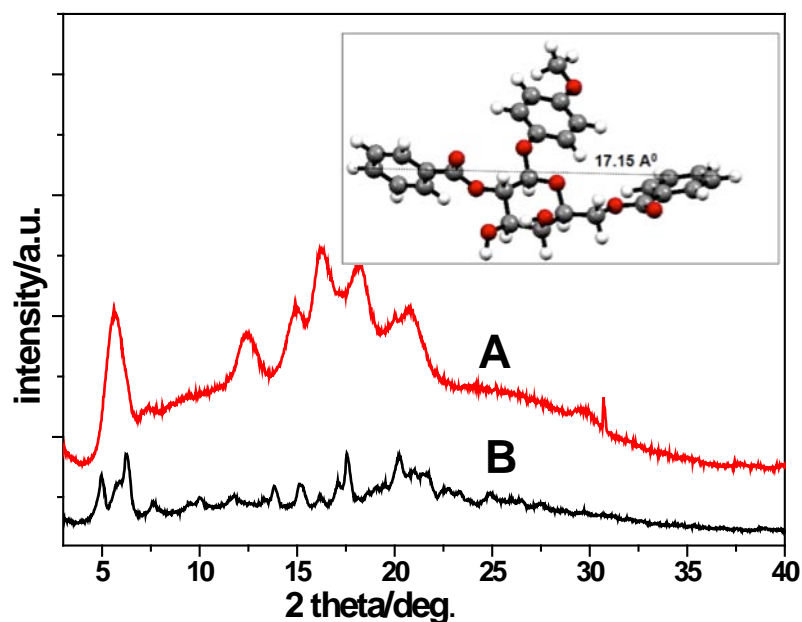


Figure S6: PXRD profiles of the xerogel in toluene **A:** 1% wt/vol and **B:** powdered compound

Table 1: Major peaks in the XRD pattern for compound 2

Compound 2	d spacing Å
xerogel	15.95,7.12,5.90,5.42,4.86,4.2,3,2.90
Powdered compound	17.66,15.12,14.11,11.59,8.76,7.61,6.66,5.82,5.48,4.39,3.90,3.80,3.52

Proof of hydrogen bonded self assembly from FTIR spectroscopy studies: Several noncovalent interaction are responsible for selfassembly in the gel state. Among those hydrogen bonding is a commonly encountered driving force for the formation of a supramolecular gels of LMOGs.⁵ FTIR measurements of the gelator in its xerogel state prepared from toluene (1% wt/vol) and powdered state were carried out in a Perkin–Elmer FTIR model RX1 spectrometer using KBr pellet. From the theoretical calculation on compound **2** we have found the presence of these stretching modes 3674 cm^{-1} and 3747 cm^{-1} for two hydroxyl group marked as ν_{α} and ν_{β} respectively (**Figure S7, II**). No such bands are present in experimental spectra (**Figure S7, I**) and no band at 3600 cm^{-1} indicates the hydrogen bond based network.⁶ FT-IR spectra of xerogel contains OH stretching frequencies at 3551 cm^{-1} , 3321 cm^{-1} , 3222 cm^{-1} and solid powder contain peaks at 3551 cm^{-1} , 3337 cm^{-1} , 3221 cm^{-1} . Peaks at the 3551 cm^{-1} stands for weakly hydrogen bonded OH stretching⁷ and other two peaks in both are the strongly intermolecular hydrogen bonded stretchings. The region ($3440\text{--}3200\text{ cm}^{-1}$) for solid powder is somewhat broadened in respect to xerogel spectra and shifts of OH stretching from 3237 to 3221 in xerogel indicates that in gel state hydrogen bonding is strengthened. When the two hydroxyl group of the gelator was protected by benzoyl groups (**3**), the compound did not gel any of the oils, indicating the significance of hydrogen bonding for the formation of supramolecular structure.

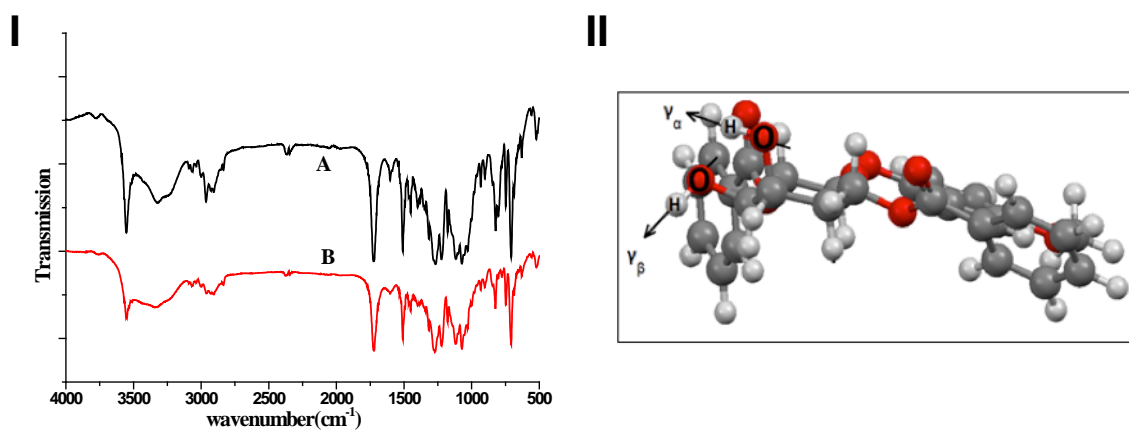


Figure S7: (I) FT-IR Spectra of (A) Xerogel in toluene 1% (wt/v) (B) and powdered compound. (II) The calculated molecular conformation of galactoside **2** together with the assigned OH stretching modes ν_{α} and ν_{β} .

5. (a) B. Escuder, S. Martl, J. F. Miravet, *Langmuir*, **2005**, *21*, 6776-6787. (b) J. H. Jung, S. Shinkai, T. Shimizu, *Chem. Eur. J.*, **2002**, *8*, 2684-2690. (c) M. Hashimoto, S. Ujiie, A. Mori, *Adv. Mater.*, **2003**, *15*, 797-800.
6. M. Bielejewski, A. Lapinski, J. Kaszynska, R. Luboradzki, J. Tritt-Goc, *Tetrahedron Lett.* **2008**, *49*, 6685-6689.
7. E. T. G. Lutz, J. H. van der Mass, *J. Mol. Struct.*, **1994**, *324*, 123-132.

Concentration dependent NMR studies: Additional evidences for intermolecular hydrogen bonding can also be obtained from ^1H NMR experiment. Concentration dependent ^1H NMR spectroscopy measurement of compound **2** in toluene- d_8 were recorded on an ECS 400 MHz (JEOL) spectrometer. The results are shown in **Figure S8**. With increasing concentration from 0.1% (wt/v) solution to 1% (wt/v) gel the two OH signal for compound **2** shifted downfield (for a 2.185 to 2.33 and for b 3.14 to 3.21) and splitted OH signals in the lower concentration becomes broad singlet in gel state. So inter molecular H-bonding is being functioning at this stage.

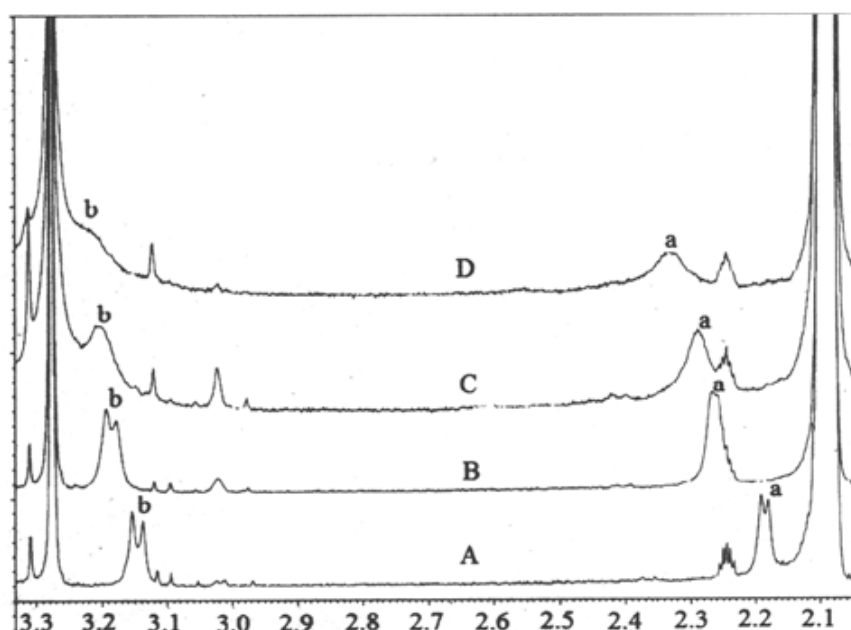


Figure S8: proton nmr of the gelator with increasing concentration (%wt/vol) (A)0.1 % (B)0.3% (C)0.6%(D)1% in toluene d_8 .

UV-Vis spectral study: UV spectroscopy measurement is an useful technique for taking information about the type of aggregation in the gel state. Concentration dependent UV measurement in toluene was done using UV/VIS spectrophotometer (varian cary). **Figure S9** showed with increasing concentration from lower (0.0003 M solution) to higher (0.02 M gel), the red shift of absorption maxima occurs (from 284 nm to 295 nm) and this indicates the possibility of j type of aggregation and here that is strating bellow gel concentration. So, it can concluded that CH- π or π - π stacking might be playing some role in aggregation of the gelator. Additionally, the calculated structure of the compound **2** (**Figure S9**) is almost flat or

planar, which may enable the compound to enjoy π - π stacking interaction to form supramolecular 3D network.⁸

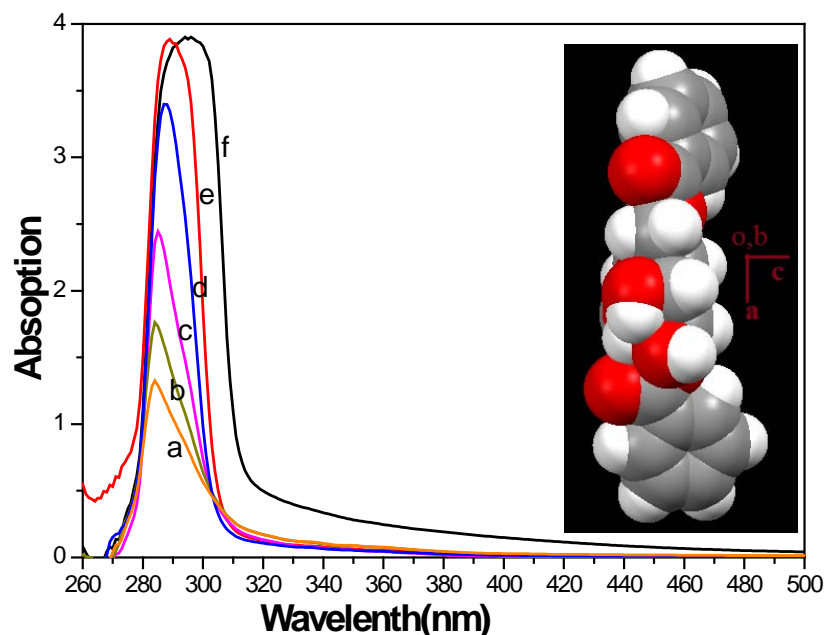


Figure S9: UV Spectra at different concentrations (a) 0.0003 M solution (b) 0.0004 M solution (c) 0.0007 M solution (d) 0.002 M solution (e) 0.004 M solution (f) 0.02 M gel

Circular Dichroism (CD) Spectra: The CD of gelator in toluene and mesitylene were recorded in Jasco J-815 spectropolarimeter, using 2 mm path length cell at wavelength 220–700 nm with a scan speed of 50 nm/min. It is known that circular dichroism (CD) comes out when the chromophoric moieties of a gelator molecule aggregate into a proper orientation. Therefore, CD spectroscopy measurements for gelator in toluene and mesitylene were performed. **Figure S10** shows that in dilute concentration (0.1% wt/v) of the gelator in toluene and mesitylene exhibited no discernible Cotton effect, but in their gel state strong CD signal was observed. Results showed in CD spectra suggesting that the chirality of the chiral center, which is far from the chromophore in the dilute solution state, possibly has moved to the chromophore as a result of gelation.⁹ and indicating that the observed CD signal in the gel state possibly originates from the chirality of the self-assembly, the gel networks rather than from the intrinsic chirality of the gelator. With reference to **Figure S10**, it can be seen that The

- (a) M. Shirakawa, S.-I. Kawano, N. Fujita, K. Sada, S. Shinkai, *J. Org. Chem.*, **2003**, *68*, 5037–5044. (b) K. Kano, K. Fukuda, H. Wakami, R. Nishiyabu, R. F. Pasternak, *J. Am. Chem. Soc.*, **2000**, *122*, 7494–7502. (c) V. Kral, F. P. Schmidtchem, K. Lang, M. Berger, *Org. Lett.*, **2002**, *1*, 51–54. (d) H. Kobayashi, A. Friggeri, K. Koumoto, M. Amaike, S. Shinkai, D. N. Reinhoudt, *Org. Lett.*, **2002**, *4*, 1423–1426.
- (a) P. F. Duan, M. H. Liu, *Langmuir*, **2009**, *25*, 8706–8713. (b) N. Yan, G. He, H. Zhang, L. Ding, Y. Fang, *Langmuir*, **2010**, *26*, 5909–5917.

toluene gel showed one positive band centered at 313 nm and one negative band at 297 nm with a shoulder band at 283 nm, but in case of mesitylene one positive band centered at 307 nm was observed, indicating that chirality of the assemblies in the two gel states are different. This results is also an indication that solvent nature plays an important role for the aggregation mode of the gelator in gel state.

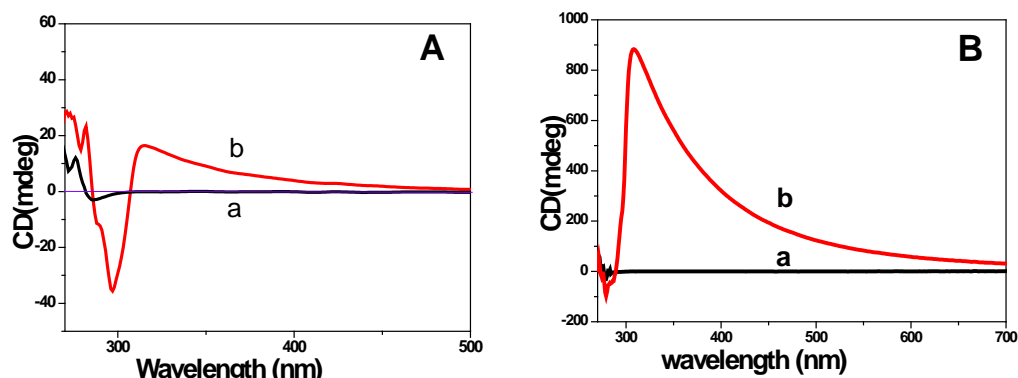


Figure S10: (A) CD spectra of gelator in toluene (a) 0.1% solution (w/v) (b) 1 % gel (w/v) (B) CD spectra of gelator in mesitylene (a) 0.1 % solution (w/v) (C) 2 % gel (w/v)

Purification of water: Removal of toxic dyes and other pollutants from contaminated water is an emerging field of research for obvious environmental reason. Removal of different toxic dyes and pollutants from waste water by suitable organogels have been reported in the literature.¹⁰ In our present work, removal of crystal violet dye from its aqueous solution can be done in two different ways. (1) Crystal violet can be removed efficiently via phase selective gelation method. To the 2 mL contaminated water, 0.5 mL of toluene was added. Then 10 mg of the compound **2** was added and heated to dissolve the gelator in toluene layer. Within 20 minutes gelator was gelled the toluene layer and after 6 hours almost all of the crystal violet was removed from aqueous layer. The dye was adsorbed in the toluene gel (see blue colour) and purified water can be collected by simple filtration. Purification efficiency was studied by UV/VIS spectrophotometer (Varian Cary) and it was 97.6% (**Figure S11; A and B**). (2) Xerogel from toluene was found to adsorbed crystal violet dye efficiently from its aqueous solution. 5 mg xerogel of gelator prepared from toluene were added to 3 mL (0.03 mM) crystal violet aqueous solution. It efficiently adsorbed the crystal violet dye from its aqueous solution and after 24 hours almost clear solution of water was

10. (a) R. Denoyel, E. S. Rey, *Langmuir* **1998**, *14*, 7321–7323. (b) S. Ray, A. K. Das, A. Banerjee, *Chem. Mater.* **2007**, *19*, 1633–1639. (c) E. Stathatos, P. Lianos, U. L. Stangar, B. Orel, *Adv. Mater.* **2002**, *14*, 354–357. (d) T. Polubesova, S. Nir, D. Zakada, O. Rabinovitz, C. Serban, L. Groisman, B. Rubin, *Environ. Sci. Technol.* **2005**, *39*, 2343–2348. (e) M. Xue, D. Gao, K. Liu, J. Peng, Y. Fang, *Tetrahedron* **2009**, *65*, 3369–3377. (f) S. Debnath, A. Shome, S. Dutta, P. K. Das, *Chem. Eur. J.* **2008**, *14*, 6870–6881.

obtained (**Figure S12B**). UV-Vis spectral study for dye adsorption shows (**Figure S12A**) that almost 96.4% dye were removed and maximum amount of crystal violet was adsorbed was 12.24 mg / gm.

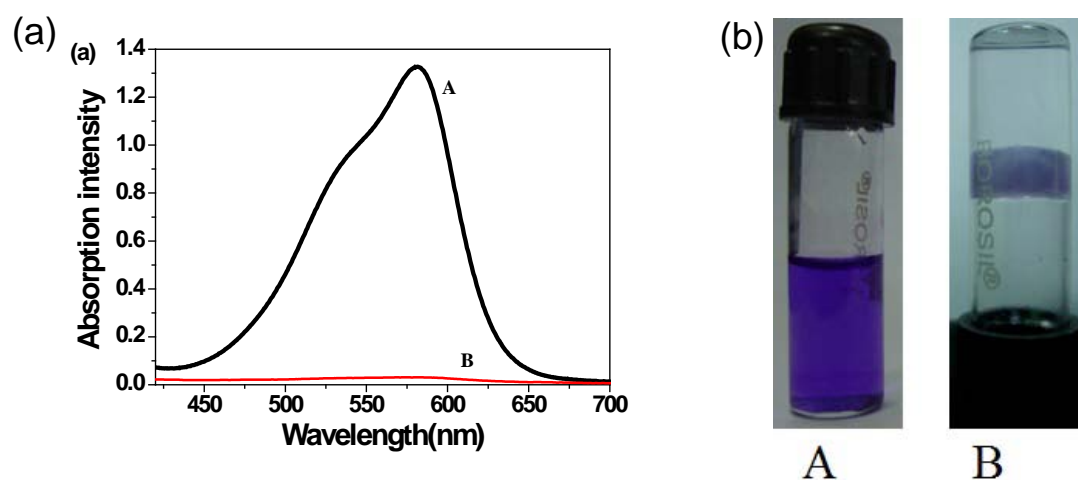


Figure S11: (a) UV-Vis study for the removal of crystal violet (A) water contaminated by crystal violet Before purification (B) after purification (Absorption maxima 583 nm) (b) Photograph of crystal violet removal via phase selective gelation.

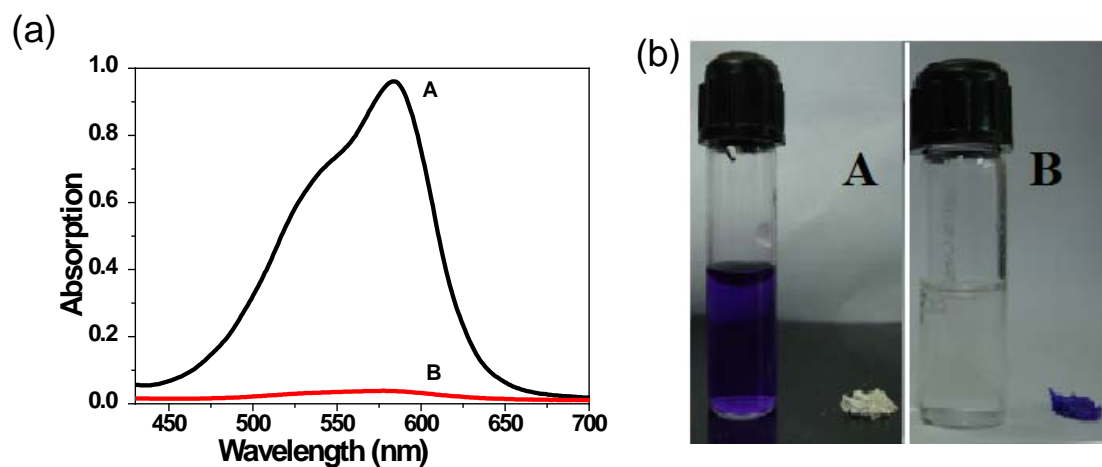


Figure S12: (a) UV-Vis spectra A) Crystal violet solution (0.03 mM) B) crystal violet solution after the addition of the xerogel (24 hours later) (b) photograph of crystal violet adsorption from water by xerogel.

Adsorption of dyes: Measured amounts of crystal violet (0.03mM) were added to each set of 3mL stock solution of buffer at pH 7.0. Then, 5 mg of xerogel of compound 1 prepared from toluene was then added to this solutions and they were left to adsorb for 24 h at room temperature without any disturbance. Then it was taken out of the solution, and the remaining dye was estimated by UV-Vis spectroscopy (**Figure S12**).

X-ray Crystallography: Crystal was mounted on a glass pip. Intensity data were collected on a Bruker's KAPPA APEX II CCD Duo system at 100 K with graphite-monochromatic Mo $K\alpha$ radiation ($\lambda = 0.71073 \text{ \AA}$). Data reduction was performed using Bruker SAINT software.^{11a} Crystal structures were solved by direct methods using SHELXL-97 and refined by full-matrix least-squares on F^2 with anisotropic displacement parameters for non-H atoms using SHELXL-97.^{11b} Hydrogen atoms associated with carbon atoms were refined in geometrically constrained riding positions. Hydrogen atoms associated with oxygen and nitrogen atoms were included in the located positions. Structure graphics shown in the figures were created using the mercury software package version 2.4. The data have been deposited at the Cambridge Crystallographic Data Center with reference number CCDC (848152).

Table S2: Crystal Data and Structure Refinement monohydrate crystal of the gelator

molecular formula	C ₂₇ H ₂₆ O ₉ , H ₂ O
molecular weight	512.49
color and habit	colorless, needle
Crystal size	0.35 x 0.45 x 0.60mm
crystal system	Orthorhombic
space group	<i>P</i> 212121 (No. 19)
unit cell parameters	(<i>a</i>) 7.313(3) Å, (α) 90.00° (<i>b</i>) 11.730(5) Å, (β) 90.00 (3)° (<i>c</i>) 29.051(10) Å, (γ) 90.00° (<i>V</i>) 2492.0(17) Å ³ , (<i>Z</i>) 4, <i>F</i> (000) = 1080
density (calcd)	1.366 g/cm ³
absorption coefficient	0.105mm ⁻¹
data collection range	-9 < <i>h</i> < 7, -14 < <i>k</i> < 14, -37 < <i>l</i> < 36; θ max 27.0°
reflections measured	total: 12935 unique (<i>n</i>): 5292 observed: 4340
no. of variables, <i>p</i>	346
R^a (for all reflections)	0.0571, 0.0404 (for observed data)
wR^b	(for all reflections) 0.1137, 0.0998 (for observed data)
GOF	0.915
Absorption correction	Multi scan
Refinement method	Full-matrix least-squares on F^2
Max. and min. Transmission	0.964 ,0.945
melting point	448 K
CCDC	848152
<i>w</i>	$1/[\sigma^2(F_o^2)+(0.0723P)^2+0.1065P]$ where $P=(F_o^2+2F_c^2)/3$

Table S3: Hydrogen Bond Geometry for G1

11. (a) SAINT Plus (version 6.45); Bruker AXS Inc.; Madison, WI, 2003. (b) SMART (version 5.625) and SHELX-TL (version 6.12); Bruker AXS Inc.; Madison, WI, 2000.

D-H...A ^a	D-H	H...A	D-A	(D-H...A)/°
O2 -- H2 .. O5 #1	0.8200	2.0300	2.785(2)	154.00
O3 -- H3 .. O10#2	0.8200	1.9200	2.739(3)	172.00
O10 -- H10A .. O9	0.91(4)	1.96(4)	2.861(3)	171(3)
O10 -- H10B .. O2 #3	0.90(4)	1.87(4)	2.767(3)	171(3)
C2 -- H2A .. O5 #3	0.9800	2.4500	3.173(3)	130.00
C4 -- H4 .. O5	0.9800	2.3000	2.698(3)	103.00
C11 -- H11 .. O9 #4	0.9300	2.5000	3.338(3)	150.00
C18 -- H18 .. O1	0.9300	2.5700	2.965(3)	106.00
C20 -- H20B .. O2	0.9700	2.5100	2.872(3)	102.00

^a Symmetry transformation code: #1= 1/2+x,1/2-y,2-z

#2 = -1/2+x,1/2-y,2-z #3 = 1+x,y,z #4 = -1+x,1+y,z

The single crystal of the gelator was obtained in its monohydrate form from (1:1) ethylacetate/hexane mixture. Detailed crystallographic data are summarised in **Table S2** and the key bond distances and angles are listed in **Table S3**. X-ray crystallography indicates the pyranose ring of the gelator remain in the typical ⁴C₁ conformation and it is orthorhombic with a = 7.41, b = 11.86, c = 29.31 and α = β = γ = 90°. Water molecule plays very important role for the crystallinity of the galactoside **2** through intermolecular hydrogen bond network. **Figure S13B** shows 1D hydrogen bond based network in which a tetrameric synthon is formed by two water molecule and two gelator molecules (marked as W1, A, W2, B) *via* these intermolecular hydrogen bonds (O10-H10A..O9, O3-H3..O10, 10-H10B..O2, O2-H2..O5). Tetrameric synthon is further extended or linked to near synthon *via* these intermolecular hydrogen bonds(O10-H10B..O2, O10-H10..O9, O10-H10B..O2) and through these intermolecular hydrogen bonds mainly mediated by water molecule, a double stranded columner type of packing arrangement is formed (**Figure S13B**). Besides O-H-O intermolecular hydrogen bondings there are also intramolecular C-H-O hydrogen bondings (listed in **Table S3**) and aromatic π-π interaction between the π ring of two tetrameric synthon of distance 3.369 Å are present. Packing along a axis shows (**Figure S14**) that in the column each molecule seems to be stacked over the same type of molecules and besides intermolecular hydrogen bondings aromatic-aromatic interaction is also present of distances 7.31 Å. **Figure S14** shows the packing viewed along a-axis in which two such columns are linked together via weak van der Waals interaction between aromatic hydrogen and sugar ring hydrogen (C24-H24-H5-C5) of distance 2.343 Å.

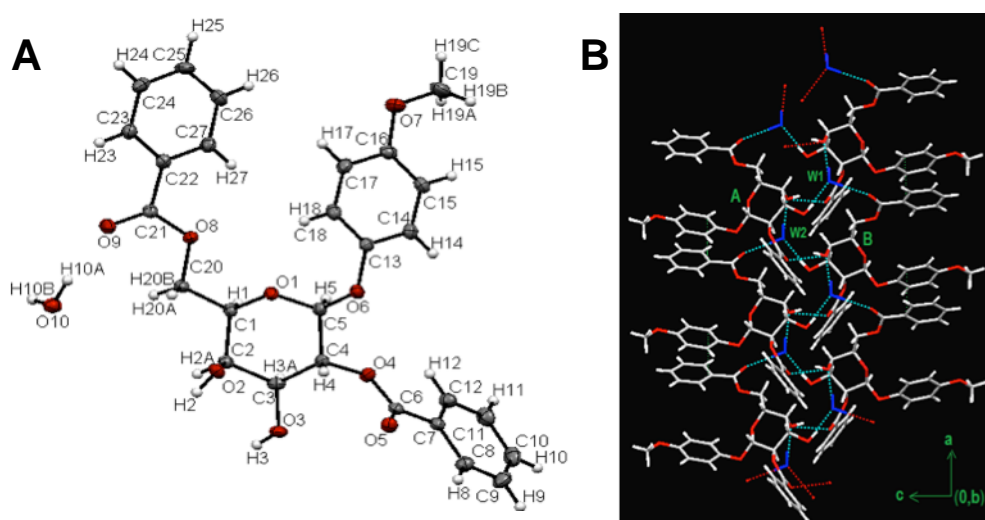


Figure S13: A: ORTEP drawing of the monohydrated compound **2** with 50% probability ellipsoids, showing the atomic numbering scheme. B: a packing view along b direction.

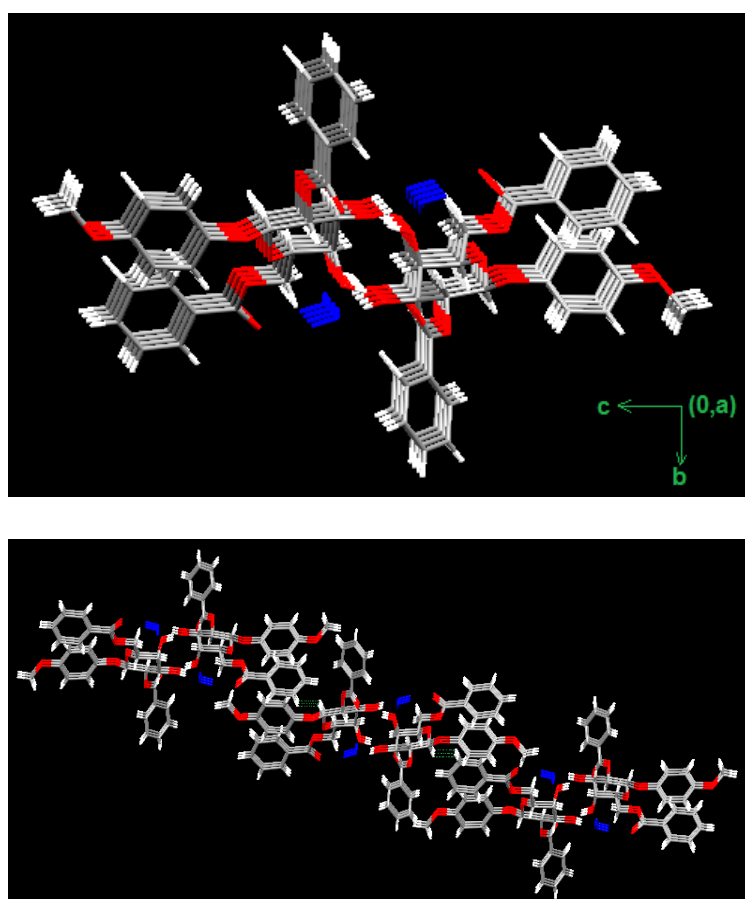


Figure S14: Crystal packing of the monohydrated compound **2** viewed along a-axis

DFT calculation: The optimized geometry and vibrational transitions of galactoside 2 were evaluated using DFT calculations on B3LYP/6-31 G(d) level¹² with GAUSSIAN 03¹³ and corresponding molecular length was estimated by measuring the distance between two farthest apart atoms.

-
12. M. J. Frisch, G. W. Trucks, H. B. Schlegel, G. E. Scuseria, M. A. Robb, J. R. Cheeseman, J. A. Montgomery, Jr., T. Vreven, K. N. Kudin, J. C. Burant, J. M. Millam, S. S. Iyengar, J. Tomasi, V. Barone, B. Mennucci, M. Cossi, G. Scalmani, G. Rega, G. A. Petersson, H. Nakatsuji, M. Hada, M. Ehara, K. Toyota, R. Fukuda, J. Hasegawa, M. Ishida, T. Nakajima, Y. Honda, O. Kitao, H. Nakai, M. Klene, X. Li, J. E. Knox, H. P. Hratchian, J. B. Cross, C. Adamo, J. Jaramillo, R. Gomperts, R. E. Stratmann, O. Yazyev, A. J. Austin, R. Cammi, C. Pomelli, J. W. Ochterski, P. Y. Ayala, K. Morokuma, G. A. Voth, P. Salvador, J. J. Dannenberg, V. G. Zakrzewski, S. Dapprich, A. D. Daniels, M. C. Strain, O. Farkas, D. K. Malick, A. D. Rabuck, K. Raghavachari, J. B. Foresman, J. V. Ortiz, Q. Cui, A. G. Baboul, S. Clifford, J. Cioslowski, B. B. Stefanov, G. Liu, A. Liashenko, P. Piskorz, I. Komaromi, R. L. Martin, D. J. Fox, T. Keith, C. Y. Al-Peng, A. Nanayakkara, M. Challacombe, P. M. W. Gill, B. Johnson, W. Chen, M. W. Wong, C. Gonzalez, J. A. Pople, GAUSSIAN 03, Revision B.05, Gaussian, Inc., Pittsburgh, PA, 2003.
13. (a) A. D. Becke, *Phys. Rev. A*, **1988**, *38*, 3098-3100. (b) A. D. Becke, *J. Chem. Phys.*, **1993**, *98*, 5648-5652. (c) C. Lee, W. Yang, R. G. Parr, *Phys. Rev. B*, **1988**, *37*, 785-789. (d) A. P. Scott, L. Radom, *J. Phys. Chem.*, **1996**, *100*, 16502-16513.